Influence of a single rib on turbulent natural convection heat transfer at a vertical flat surface

Dong-Gyu Lee and Bum-Jin Chung
Department of Nuclear Engineering, Kyung Hee University
#1732 Deogyeong-daero, Giheung-gu, Yongin-si, Gyeonggi-do, 17104, Korea
Corresponding author: bjchung@khu.ac.kr

***Keywords : Ribbed surface; Natural convection; Roughness effect**

1. Introduction

At the early stage of Small Modular Reactor (SMR) accident, core cooling is provided by various safety systems like Passive Containment Cooling System of i-SMR. However, ultimate heat sink relies on the natural convection cooling at the outer surface of the SMR steel containment vessel (CV). This allows for long-term core cooling without the need for external driving force.

In practice, heat transfer surfaces (Outer surface of CV) may include pipes, flanges, and manways, which can act as obstacles or surface roughness to natural convection heat transfer. Surface roughness can significantly enhance heat transfer by disrupting the near-wall thermal boundary layer, particularly the viscous sublayer [1]. In contrast, roughness can also obstruct the flow and induce a recirculation region, which can reduce heat transfer. Therefore, it is necessary to examine the effects of roughness on wall heat transfer in detail.

In studies of flat-plate flows, roughness effects are commonly modeled using ribs. The influence of ribs to near-wall forced flow were summarized by Prasad and Saini (1988) [2]. They reviewed general phenomenology of the viscous sublayer in forced convection duct flows with surface ribs. Fig. 1 illustrates the flow patterns of the viscous sublayer according to relative roughness. The relative roughness is defined as p/e, where p is the rib pitch (spacing) and e is the rib height.

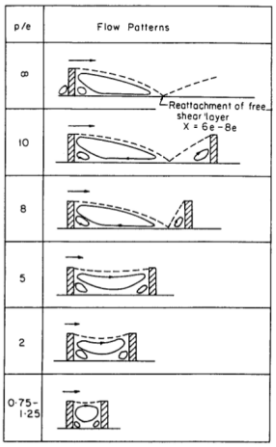

Fig. 1. Flow patterns according to relative roughness (p/e).

When the flow encounters a rib, recirculation regions form upstream and downstream of the rib. The flow separates at the top of the rib, and the separated shear layer reattaches to the surface downstream of the rib. Heat transfer tends to decrease in the vicinity of the recirculation region, whereas it increases near the reattachment point. The influence of the rib depends on its size relative to the viscous sublayer [3].

In natural convection, studies on flat plate ribs have been conducted mainly in the laminar regime. Bhavnani and Bergles (1990) reported that in the regions between ribs, local heat transfer enhancement was observed, which they associated with boundary layer reattachment [4]. However, heat transfer decreased compared with a plain surface, regardless of rib size.

Overall, rib studies in natural convection have been extensive in the laminar regime, whereas studies in the turbulent regime remain limited (e.g., Ahmed and Tanda, 2024; Tanda, 2008; Tanda et al., 2023) [5-7]. However, on the CV surface, natural convection flow occurs at very large scales. The flow is turbulent and corresponds to a high Rayleigh number regime (High Ra).

Moreover, most existing work has focused on repeated rib configurations, and thus detailed investigations of rib induced local phenomena are still scarce. To provide general phenomenology of rib induced heat transfer changes in turbulent natural convection, the present study performed experiments with a single rib and examined the effect of rib height by varying the rib size. To achieve high Ra turbulent natural convection conditions using a small scale apparatus, we employed the heat and mass transfer analogy. Using a copper sulfate–sulfuric acid electroplating system, Ra on the order of 10^{14}–10^{15} can be achieved. In this study, local heat transfer upstream and downstream of a single rib was measured and compared with that over a plain surface.

2. Experimental setup

2.1 Methodology

Heat and mass transfer systems are analogous, as the governing equations for the two phenomena are identical [8]. Therefore, by employing the analogy concept, heat transfer experiments can be conducted as mass transfer experiments. In this study, a copper sulfate-sulfuric acid ($CuSO_4$-H_2SO_4) electroplating system was used to simulate natural convection heat transfer. When electric potential is applied between the electrodes, cupric ions which released at anode are plated at cathode. As this reaction proceeds, concentration of cupric ions near the cathode decreases. The difference of cupric concentration induce buoyancy and generate natural convective flow at near the cathode The rate at which cupric ions deposit onto the cathode reflects the mass transfer rate, which corresponds to the heat transfer rate. To measure the mass transfer near the cathode without directly sampling the ion concentration, a limiting current technique was employed. The physical properties were calculated using the correlation conducted by Fenech and Tobias [9]. The mass transfer coefficient (h_m) followed as:

$$h_m = \frac{\left(1-t_{Cu^{2+}}\right) I_{lim}}{nF\Delta C} \left(\Delta C = C_b\right). \qquad (1)$$

More details of this technique can be found in the work of [10, 11].

2.2 Experimental apparatus

Figure 3 shows a photograph of the experimental apparatus and the electrode with the attached rib. The reservoir has a height of 2.4 m and a width of 0.4 m, providing an open-pool configuration in which the flow developing along the electrode is not disturbed by the reservoir walls. The cathode and anode face each other.

To measure local heat transfer, the cathode was electrically segmented into piecewise sections. In particular, to measure local heat transfer more finely upstream and downstream of the rib, we installed a more densely segmented piecewise electrode (hereafter referred to as the test electrode). The test electrode was segmented at 6 mm intervals, and the thickness of the insulating layer between adjacent segments was 0.5 mm, which is negligible. The single rib was attached to the test electrode.

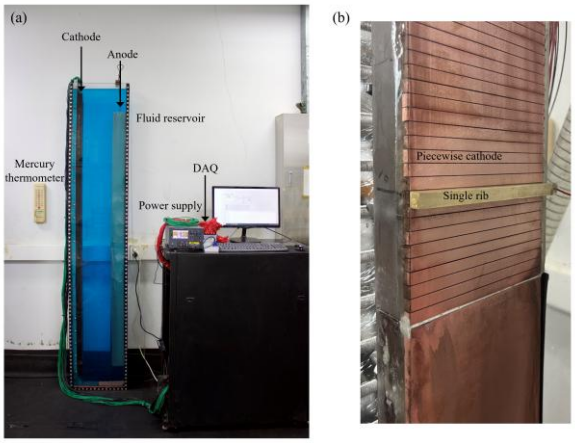

Fig. 3. Experimental setup: (a) Test apparatus; (b) Piecewise electrode with single rib.

All current and voltage were measured using a National Instruments (NI) data acquisition (DAQ) system. Electrical current and voltage were measured using NI-9247 and NI-9225 modules, respectively.

2.3 Test matrix

Figure 2 schematically illustrates the rib geometry used in the present study and defines the governing parameters. The rib has a square cross section, and e denotes the rib height. Here, δ represents the thickness of the viscous sublayer. For forced convection duct flows, relative roughness is also expressed as e/D, where D is the duct diameter [3]. Here, D represents the characteristic length scale of the flow. In natural convection, however, the characteristic length scale is more appropriately related to the boundary layer thickness. Therefore, in the present study, the relative roughness is expressed as e/δ.

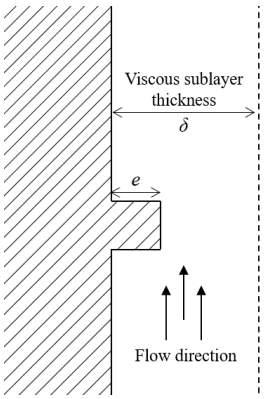

Fig. 2. Schematic of the parameter for single rib surface.

Table 1 presents the test matrix of the present study. The single rib was installed in the region where Grashof number, $Gr_H > 10^{10}$, in which turbulent natural convection is characterized by an approximately constant heat transfer [12, 13]. Following the present methodology, the rib was placed at $Ra_H = 3.1\times10^{14}$, corresponding to $H = 1.235$. The working fluid used in this study has Prandtl number, $Pr = 2{,}094$.

Table 1. Test matrix.

Ra_H	Gr_H	Pr	δ (mm)	e/δ	e (mm)
3.1×10^{14}	1.5×10^{11}	2094	6	2	3
				1	6
				0.75	8

Because no established correlation is available to estimate the viscous sublayer thickness in turbulent natural convection, we estimated the viscous sublayer thickness using existing heat transfer correlations together with scaling arguments from turbulent forced convection [8].

$$Nu_x = 0.164 Gr_x^{1/3} Pr^{2/9}. \quad (2)$$

$$\delta_t \sim \frac{H}{Nu}. \quad (3)$$

$$\delta_v \sim \delta_v Pr^{1/3}. \quad (4)$$

The estimated viscous-sublayer thickness is approximately 6 mm. Based on $\delta = 6$ mm, the rib height was selected to yield $e/\delta = 2$, 1, and 0.75. Accordingly, e was set to 3, 6, and 8 mm.

3. Results and discussions

3.1 Comparison of experimental results with existing study

Figure 4 compares the present averaged Nusselt number (Nu_{avg}) with the existing correlations. Original ranges of correlations are indicated by solid lines, and the extrapolated ranges are indicated by dashed lines. The correlations of Churchill and Chu [14] and of Eckert and Jackson [15] were extrapolated for $Ra_x > 10^{12}$.

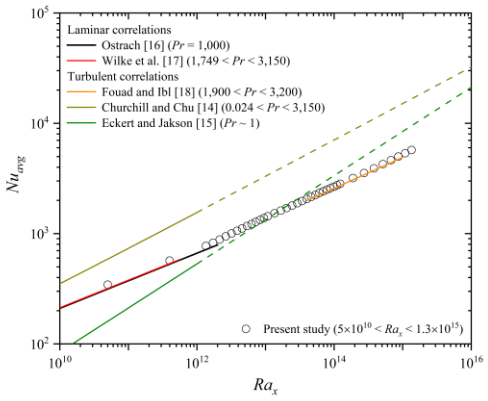

Fig. 4. Comparison of experimental results and existing studies [14-18].

For the laminar flow regime ($Ra_x < 1.3\times10^{12}$), the experimental data agreed well with Ostrach's correlation developed for very large Pr, within a maximum relative error of 8.3 % [16]. For the turbulent flow regime ($Ra_x > 4.0\times10^{13}$), the experimental results agreed with the turbulent correlation of Fouad and Ibl within a maximum relative error of 7.0 % since this correlation was developed from mass transfer experiments, as in the present study [18]. However, the correlations of Churchill and Chu [14] and Eckert and Jackson [15] showed large deviations from the present experimental results. The discrepancies from existing correlations in the turbulent regime are attributed to the large difference between their development ranges and the Pr range of the present study, whereas the present data agree well with studies that employed the same experimental methodology.

3.2 Influence of single rib on turbulent natural convection

Figure 5 shows how the Nu_{avg} measured in test electrode changes with increasing e. The horizontal axis is e, where $e = 0$ corresponds to the base case, and the vertical axis is the Nu_{avg}. The characteristic length was taken as the length of the test electrode ($H = 0.216$ m). "Overall" denotes the Nu_{avg} evaluated over the entire test electrode, including the rib.

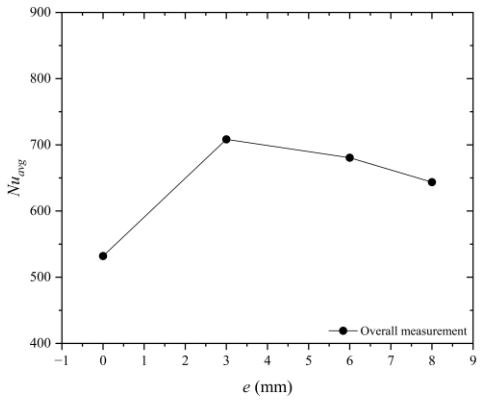

Fig. 5. Influence of the rib according to relative location.

For the overall data, heat transfer first increases with increasing e and then decreases. The maximum heat transfer occurs at e = 3 mm. For e = 6–8 mm, the heat transfer decreases. The fact that heat transfer improves and then decreases as e increases is different from the phenomenon commonly known in forced convection. This suggests that the larger ribs may have weakened the driving force of the flow near the wall, because of forming a wider recirculation zone.

Overall, the average heat transfer is enhanced relative to the base case. This differs from laminar natural convection, because turbulent diffusion promotes early reattachment and suppresses the development of a downstream recirculation region.

3.3 Local heat transfer characteristics with a single rib on turbulent natural convection

Figure 6 presents the local heat transfer coefficient as a function of Ra_x. The rib is located at approximately $Ra_x = 3.5\times10^{14}$. The data measured at the rib location are indicated by the black vertical dashed line. The black symbols represent the heat transfer results for the base (plain) surface. For the base case, the heat transfer coefficient remains nearly constant with Ra_x, which is a characteristic of turbulent natural convection [12, 13].

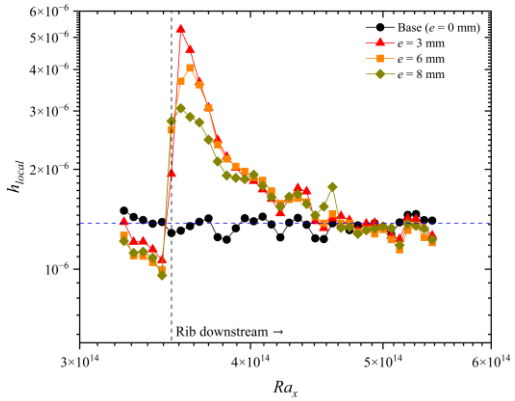

Fig. 6. Local heat transfer characteristics of surface with single rib.

In all ribbed cases, the heat transfer coefficient decreases as the flow approaches the rib in upstream of the rib. The rib blocks the flow, and forms recirculation flow. If e increases in rib upstream, the heat transfer decreases. This is because as e increases, the rib decelerates the flow near the wall more strongly.

For the data measured only at the rib location, heat transfer is improved compared to the base. The ribs protrude further outward than the viscous sublayer near the wall, so they encounter more of the cold fluid. When the e increases, heat transfer increases monotonically at the rib. This is because a taller rib provides greater interaction with fresh fluid outside the boundary layer.

Immediately downstream of the rib, the heat transfer increases sharply, reaching a peak just after the rib. This enhancement is attributed to rapid boundary layer reattachment, which supplies fresh fluid to the wall. After reattachment, the boundary layer redevelops and the heat transfer coefficient gradually decreases, eventually approaching the base surface level.

Although e increases, the heat transfer downstream of the rib decreases. The maximum heat transfer occurs at e = 3 mm, which suggests that recirculation induced by the rib is limited while the viscous sublayer is sufficiently disturbed. For e = 6–8 mm, the heat transfer decreases because the effect of the flow recirculation becomes larger than the effect of the sublayer disruption.

3.4 Influence of ratio of flow distance and rib height (x/e)

Figure 7 shows the normalized form of the data presented in Fig. 6. The horizontal axis is downstream distance x normalized by the rib height e, and the vertical axis is normalized by the base (plain surface) value. A value of 1 on the vertical axis indicates the same heat transfer level as the base case.

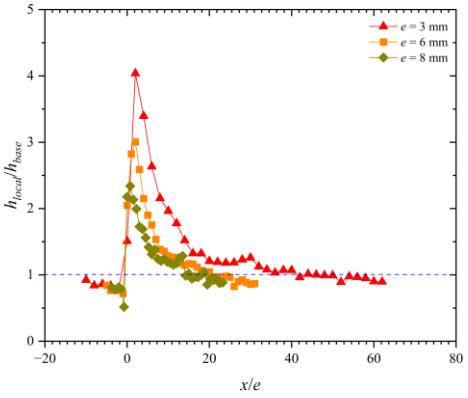

Fig. 7. Normalized local heat transfer coefficients of surface with single rib.

Immediately downstream of the rib, heat transfer increases due to flow reattachment. The reattachment occurs at approximately $x/e \sim 2$–4. In previous studies on laminar natural convection, although not explicitly stated, the experimental data suggest that reattachment occurs at $x/e \sim 3$–5 [4]. The present results show a similar trend to those laminar natural convection studies. However, present study indicates a shorter reattachment length in turbulent natural convection than typical values reported for forced convection (about 7) [2].

A plausible explanation is presented by Fig. 8. It shows that the downstream recirculation region tends to move upward, which intensifies the adverse pressure gradient near the rib (under mass conservation) and promotes early reattachment. In other words, as the recirculation flow rapidly escapes upward under its own buoyancy, the reattaching flow fills the vacated region.

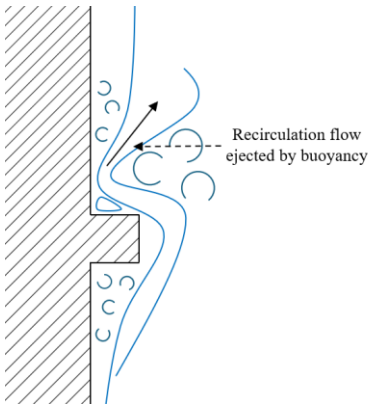

Fig. 8. Schematic of the flow pattern on natural convection with single rib.

4. Conclusions

This study experimentally measured the local natural convection heat transfer characteristics induced by a single rib attached to a vertical wall. By employing the heat and mass transfer analogy, high *Ra* turbulent natural convection was reproduced using a small scale apparatus, and the rib effects were quantified under these conditions.

While previous natural convection rib studies have been largely limited to the laminar regime, the present study examined the influence of a single rib in the turbulent regime and obtained the following findings: (1) upstream of the rib, heat transfer decreases as the flow approaches the rib due to the formation of a rib-induced recirculation region; (2) heat transfer increases sharply at the rib because the rib disrupts the viscous sublayer; (3) unlike forced convection, turbulent natural convection exhibits boundary layer reattachment immediately downstream of the rib; and (4) cases with $e/\delta < 1$ showed greater heat transfer enhancement than the plain surface, indicating that the rib primarily disturbed the viscous sublayer without causing substantial flow blockage and recirculation flow.

The single rib heat transfer characteristics reported in this study are expected to provide fundamental reference data for future investigations of heat transfer over repeated rib structures in turbulent natural convection. In future work, the flow field around a single rib will be measured using Particle Image Velocimetry (PIV).

5. Acknowledgements

This work was supported by the Innovative Small Modular Reactor Development Agency grant funded by Korea Government Ministry of Climate, Energy and Environment (MCEE) (No. RS-2024-00404240).

REFERENCES

[1] Webb R.L., Kim N., Enhanced heat transfer, Taylor &amp, (2005).
[2] Prasad B., Saini J., Effect of artificial roughness on heat transfer and friction factor in a solar air heater, Solar energy, 41 (1988) 555-560.
[3] Dawson D.A., Trass O., Mass transfer at rough surfaces, International Journal of Heat and Mass Transfer, 15 (1972) 1317-1336.
[4] Bhavnani S.H., Bergles A.E., Effect of surface geometry and orientation on laminar natural convection heat transfer from a vertical flat plate with transverse roughness elements, International Journal of Heat and Mass Transfer, 33 (1990) 965-981.
[5] Ahmed E.N., Tanda G., An experimental and numerical study of laminar natural convection along vertical rib-roughened surfaces, International Journal of Heat and Mass Transfer, 223 (2024) 125227.
[6] Tanda G., Natural convective heat transfer in vertical channels with low-thermal-conductivity ribs, International journal of heat and fluid flow, 29 (2008) 1319-1325.
[7] Tanda G., Ahmed E.N., Bottaro A., Natural convection heat transfer from a ribbed vertical plate: effect of rib size, pitch, and truncation, Experimental Thermal and Fluid Science, 145 (2023) 110898.
[8] Bejan A., Convection heat transfer, John wiley & sons, 2013.
[9] Fenech E.J., Tobias C.W., Mass transfer by free convection at horizontal electrodes, Electrochimica acta, 2 (1960) 311-325.
[10] Shin D.-H., Lee D.-G., Chung B.-J., Measurements of natural convective heat transfer of the inclined torus, International Journal of Heat and Mass Transfer, 217 (2023) 124729.
[11] Park S.-Y., Park D.-H., Chung B.-J., Natural convection experiments around an upper dome varying Rayleigh number and truncation angle, Experimental Thermal and Fluid Science, 169 (2025) 111548.
[12] Tsuji T., Nagano Y., Characteristics of a turbulent natural convection boundary layer along a vertical flat plate, International journal of heat and mass transfer, 31 (1988) 1723-1734.
[13] Nakao K., Hattori Y., Suto H., Takimoto H., Niida Y., Scaling high Rayleigh number natural convection boundary layer statistics: A vertical water tunnel experiment, Physics of Fluids, 35 (2023).
[14] Churchill S.W., Chu H.H., Correlating equations for laminar and turbulent free convection from a vertical plate, International journal of heat and mass transfer, 18 (1975) 1323-1329.
[15] Eckert E.R.G., Jackson T.W., Analysis of turbulent free-convection boundary layer on flat plate, in, 1950.
[16] Ostrach S., An analysis of laminar free-convection flow and heat transfer about a flat plate parallel to the direction of the generating body force, in, 1952.

[17] Wilke C., Eisenberg M., Tobias C., Correlation of limiting currents under free convection conditions, Journal of the electrochemical Society, 100 (1953) 513-523.
[18] Fouad M., Ibl N., Natural convection mass transfer at vertical electrodes under turbulent flow conditions, Electrochimica Acta, 3 (1960) 233-243.